

Quasicrystals in a Monodisperse System

Anna Skibinsky^{1,2}, Sergey V. Buldyrev¹, Antonio Scala¹,
Shlomo Havlin^{1,3}, H. Eugene Stanley¹

¹*Center for Polymer Studies and Department of Physics,
Boston University, Boston, MA 02215, USA*

²*Department of Chemistry, Boston University, Boston, MA 02215, USA*

³*Department of Physics, Bar-Ilan University, Ramat-Gan 52900, Israel*

(February 5, 2020)

We investigate the formation of a two-dimensional quasicrystal in a monodisperse system, using molecular dynamics simulations of hard sphere particles interacting via a two-dimensional square-well potential. We find that more than one stable crystalline phase can form for certain values of the square-well parameters. Quenching the liquid phase at a very low temperature, we obtain an amorphous phase. By heating this amorphous phase, we obtain a quasicrystalline structure with five-fold symmetry. From estimations of the Helmholtz potentials of the stable crystalline phases and of the quasicrystal, we conclude that the observed quasicrystal phase can be the stable phase in a specific range of temperatures.

I. INTRODUCTION

Stable quasicrystalline phases are typically found in binary mixtures [1], where the various arrangements of the two components contribute to the degeneracy of the local environments [2], allowing a quasicrystalline phase to be entropy stabilized [3]. With one notable exception [4], previous studies did not support the existence of a stable quasicrystalline phase in a monodisperse system [5,6].

We study a simple model that allows us to estimate the crystal and quasicrystal entropies and thereby study the Helmholtz potentials of the crystals and quasicrystal. The ground state of this system is a periodic crystal, yet we explore the possibility that the quasicrystalline configuration is the equilibrium state in a certain temperature regime. Although quasicrystals do not have short range order, they do have recurring local environments that, in our model, resemble the basic cells of the stable crystalline phases. From the entropies of the stable crystalline phases and by estimating the configurational entropy of the quasicrystal, we infer that the quasicrystal may be an equilibrium state. We observe sharpening of five fold diffraction peaks when the starting amorphous phase is annealed. In two dimensions, five fold diffraction peaks pertain to crystallographically disallowed point groups which characterize quasicrystals [7].

II. MD METHODS

To study quasicrystalline stability in a monodisperse system, we perform molecular dynamics (MD) simulations of a two-dimensional model of hard spheres interacting with an attractive square-well (SW) potential [Fig. 1]. The simplicity of this SW potential allows us to study the fundamental characteristics of the system. By tuning the width of the SW potential, we can control the local geometric configurations formed by the particles. The structures of the crystalline and quasicrystalline phases can thus be clearly defined and analyzed.

We perform MD simulations in the NVT ensemble, using a standard collision event list algorithm [8] to evolve the system, while we use a method similar to the Berendsen method to achieve the desired temperature [9]. The depth of the potential well is $\epsilon = -1.0$. Energies are measured in units of ϵ , temperature is measured in units of energy divided by the Boltzmann constant, ϵ/k_B , and the mass of the particle is $m = 1$. We choose the value of the hard core distance to be, $a = 10$, and the ratio of the attractive distance b to the hard core distance a , to be $b/a = \sqrt{3}$. Since the diagonal distance between two corners of a square is $\sqrt{2}$ times the

length of one side, choosing $b/a = \sqrt{3}$ favors the formation of a square crystal lattice where each particle interacts with 8 neighbors [Fig. 2a]. This constraint inhibits the formation of a triangular crystal, which would form at low temperatures if $b/a > \sqrt{3}$ or at high densities.

III. CRYSTAL AND AMORPHOUS PHASES

Studying the behavior of the system at low temperatures we observe the formation of local structures similar to that shown in Fig. 2. These structures constitute local environments [2] that can reproduce crystallographically allowed symmetry if translationally ordered. First, we consider the stable periodic crystal phases produced by translationally ordering each of the configurations in Fig. 2 and calculate the energies of these crystal structures at $T = 0$. In our system, the two allowed local configurations are the 4-particle square and the 5-particle pentagon (indicated by the symbol “P” in Fig. 2b,c). Particles form these two geometries because the nearest neighbor diagonal and adjacent distance between particles in these configurations is less than $b/a = \sqrt{3}$, the SW width. Four particle squares make up the square crystal; since each particle has 8 neighbors, at $T = 0$, the potential energy per particle is $U_{sq} = -4.0$. Pentagons do not tile the plane; however, the formation of two kinds of crystals based on the local five particle pentagon is possible. In the type I pentagonal crystal, each crystalline cell consists of 5 particles, one of which has 8 neighbors and four of which have 9 neighbors; hence, $U_{pI} = -4\frac{2}{5}$ [Fig. 2b]. In the type II pentagonal crystal, each crystalline cell consists of 6 particles, two of which have 8 neighbors and 4 of which have 9 neighbors; hence, $U_{pII} = -4\frac{1}{3}$ [Fig. 2c]. Since $U_{pI} < U_{pII} < U_{sq}$, at our chosen density and low enough temperatures, the type I pentagonal crystal should be the stable phase at $T = 0$ [Fig. 3].

Next, we investigate the stability of the three crystalline phases at $T > 0$ by estimating the Helmholtz potential per particle $A = U - TS$ in the square crystal and in the pentagonal crystals of type I and type II. Here S is the entropy. Since our simulations are performed at constant density, we must use the Helmholtz potential instead of the Gibbs potential. We

study the system at dimensionless number density $\rho = a^2 N/V \equiv 0.857$. We have simulated a square crystal with $N=961$, a pentagonal crystal type I with $N=1040$, and a pentagonal crystal type II with $N=792$, all at the same ρ . We checked that at low temperatures, $T < 0.1$, the potential energy $U(T)$ is temperature independent, and has the same value as the potential energy of the ideal crystal at $T = 0$. Hence, we approximate $U(T)$ at higher T by $U(0)$.

In order to plot the behavior of the Helmholtz potentials of the three crystals for $T < 0$, we find the entropic contributions S , by estimating the entropy per particle for each of the three crystal types. We use the probability density $p(x, y)$ to find a particle at position x, y , where the average is taken over every particle in the crystalline cell:

$$S = \left\langle \int p(x, y) \ln p(x, y) dx dy \right\rangle_{cell}. \quad (1)$$

We estimate $p(x, y)$ by the fraction of the total time t spent by a particle in a discretized area, $\Delta x \Delta y$, at a low enough temperature that the potential energy fluctuations of the crystalline structure are negligible. The values of the entropies for the three crystals are given in Table I.

Our estimates for the temperature dependence of the Helmholtz potential for the three types of crystals are given in Fig. 3. The condition for stability of the pentagonal crystals is that their Helmholtz potentials, A_{pI} and A_{pII} , are lower than the Helmholtz potential of the square crystal, A_{sq} . In accord with this condition, the square crystal is stable at temperatures above $T = 0.203$, the type II pentagonal crystal is stable between $T = 0.195$ and $T = 0.203$ and the type I pentagonal crystal is stable below $T = 0.195$.

While studying the interesting region around $T \approx 0.2$ (see Fig 3), we observe the formation of the quasicrystal. We choose to investigate, using MD simulations, our system at $T \approx 0.2$ because this is the temperature regime where the three crystals have similar values of Helmholtz potential. Cooling the fluid phase, we find the formation of the square crystal below $T \approx 0.5$. However, when further cooled into the temperature regime where the Helmholtz potentials of the two pentagonal crystals are lower than the Helmholtz potential

of the square crystal, the system does not form pentagonal crystal I or pentagonal crystal II (within our simulation times), but remains as the square crystal. Hence, we use a different approach to try to form the pentagonal crystals: we heat an amorphous phase. We first form the amorphous phase by quenching the system from high to very low temperatures $T \leq 0.1$. To do this, we study a system of $N = 961$ [10] particles at $\rho = 0.857$ which is initially in the fluid phase at high temperature, $T = 10$. We quench this system to $T = 0.1$ and thermalize for 10^7 time units [11]. Time constraints prevent us from studying systems with more than 961 particles. Long thermalization times are required to stabilize thermodynamic observables like energy and pressure.

The amorphous phase is a homogeneous mixture of pentagons and squares [Fig. 4a]. The lack of long range structural order in the amorphous phase is evident from the homogeneity of the circles in the isointensity plot [Fig. 4b]. When heating the amorphous phase [12] to temperatures above $T \approx 0.15$, we find that diffusion becomes sufficient for local rearrangement to occur, and the pentagons begin to coalesce. Instead of forming type I or II pentagonal crystals, the pentagons begin to form rows [Fig. 4c] that bend at angles which are multiples of 36° . The angle in the bending of the rows gives rise to the five-fold orientational symmetry, which corresponds to the ten easily observed peaks in the isointensity plot [Fig. 4d]. These 10 peaks are characteristic of the quasicrystal phase [13], as they are arranged with disallowed fifth order point group symmetry [7]. The configuration that we obtain has defects, mainly patches of square crystal, which cause the discontinuity in the rows and lead to the broadening of the diffraction peaks. For comparison, we present in Fig. 5 the isointensity plots of the simulated square and pentagonal crystals. The diffraction patterns illustrate the symmetry of the original crystal system. The four equal sides of the square crystal unit cell (Fig 2a) are clear in the symmetry of the isointensity plot Fig. 5. In the isointensity plot of pentagonal crystal I (Fig. 5b), the central region which corresponds to the long range order, shows no hints of anything but well defined centered-rectangular symmetry (Fig 2b) [14]. The isointensity plot of pentagonal crystal II has mainly a rectangular symmetry that matches the rectangular symmetry of the unit cells (Fig 2c). Although

the two pentagonal crystals are formed from ordered pentagons, their long range symmetries are four sided. Their corresponding isointensity plots illustrate these four fold symmetries which are distinctly different from the five fold quasicrystal isointensity plot.

IV. QUASICRYSTAL

A. Formation

Since the phase transition between the two pentagonal crystals occurs at $T \approx 0.2$, we choose this temperature as the one to investigate for quasicrystal formation. Annealing the system at $T = 0.205$, we equilibrate the amorphous phase, initially at $T = 0.1$, for 2×10^7 time units, and calculate the diffusion coefficient D , pressure P [15] and potential energy U . We calculate D using the Einstein relation $D = \frac{1}{2d} \lim_{t \rightarrow \infty} \frac{\langle \Delta r(t)^2 \rangle}{t}$, where d is the system dimension. After a short initial period of increase, we observe that D and U decrease with time and reach plateaus [Fig. 6]. The diffusion coefficient approaches zero, which is consistent with the possible formation of a quasicrystal phase. The isointensity peaks also sharpen with the duration of annealing. Due to MD time constraints, we are not sure that we reach the potential energy of a perfect quasicrystal, which is expected to be comparable to the energies, $U_{pI} = -4\frac{2}{5}$ and $U_{pII} = -4\frac{1}{3}$, of the pentagonal crystals. The lowest potential energy reached is $U_{qc} = -4.25$.

We observe the spontaneous formation of the quasicrystal phase in the range of temperatures between $T = 0.190$ and $T = 0.205$. As we heat either the amorphous phase or the quasicrystal above $T = 0.21$, the square crystal forms, consistent with the Helmholtz potential estimations of Fig. 3.

Next we address the question of whether the quasicrystal phase is stable, by comparing the values of the Helmholtz potential for the three crystal types. As can be seen [Fig. 4c,d], the structure of the quasicrystal arises from the bending rows of pentagons which locally resemble the pentagonal crystals of either type I or II. We assume that local arrangements

of particles corresponding to a square crystal are defects [16] that would be absent in the perfect quasicrystal. If we assume that the local arrangement of the quasicrystal is similar to a combination of the local arrangements in the pentagonal crystal I and the pentagonal crystal II, we can approximate the Helmholtz potential of the quasicrystal by the average Helmholtz potential of the two pentagonal crystals. Because the quasicrystals have a positive entropy contribution to the total entropy due to their degeneracy [3], we add an additional term $-TS_c$ to the original estimate of the Helmholtz potential energy. Here S_c is the entropy due to the possible configurations of the quasicrystal.

B. Entropy

We estimate S_c as the logarithm of the number of configurations formed by n pentagons in the quasicrystal. A single pentagon can be oriented in two possible ways when attached side by side to an existing row of pentagons. Neglecting the interaction between adjacent rows, we can estimate the upper bound for the number of configurations as 2^n , where n is the total number of pentagons in the quasicrystal. Note that at point A on Fig. 3, the Helmholtz potentials of both pentagonal crystals coincide, so an additional $-TS_c$ term should stabilize the quasicrystal in the vicinity of point A.

To better estimate S_c , we notice that the bending rows of pentagons forming the quasicrystal resemble a compact self-avoiding random walk on the hexagonal lattice. The number of such walks grows as Z^n where $Z \approx 1.3$ and n is the number of steps [17]. Since the formation of one pentagon in the midst of a perfect square crystal lowers the energy of the system by $U = -1$, we estimate n to be $(U_{qc} - U_{sq})N$. Assuming that the ground state energy of the quasicrystal is between U_{pI} and U_{pII} , the number of pentagons in the quasicrystal, should not be smaller than the number of pentagons in the crystal of type II (which is the pentagonal crystal with the lesser number of pentagons and has $n = \frac{1}{3}N$). We estimate the entropy of configuration per particle to be $S_c \approx \ln(Z^n) = \frac{1}{3}\ln(1.3) = 0.087$. Thus, the quasicrystal should be more stable than the pentagonal crystals between $T = 0.16$

and $T = 0.23$, where the gap between the Helmholtz potential of the pentagonal crystals is smaller than the configuration term TS_c which ranges from 0.014 to 0.020 in the interval where T increases from 0.16 to 0.23. Since the TS_c term lowers the Helmholtz potential of the obtained quasicrystal configuration below the Helmholtz potentials of the two pentagonal crystals, it is likely that the obtained state with five-fold rotational symmetry is not the coexistence of type I and II pentagonal crystals, but is a stable quasicrystalline phase. A more rigorous investigation of this problem would require the construction of a Penrose type tiling [18] involving crystals of type I and II.

V. DISCUSSION

To summarize, perfect pentagonal crystals of type I and II do not form spontaneously during the time scales of our study. Instead, the quasicrystal, having long-range, five-fold orientational order with no translational order, forms from the coalescence of pentagonal units present in the starting amorphous phase. The starting amorphous configuration must initially be quenched at a low enough temperature in order to prevent crystallization to the square phase. Moreover, the amorphous phase must be carefully thermalized as we have observed that, upon heating a poorly equilibrated amorphous phase with a higher concentration of squares, the system phase separates into regions of pentagons and squares. If the starting amorphous phase does not have a sufficient concentration of pentagons, the quasicrystal will not form. In addition, large regions of square crystal will inhibit the long range order of pentagons and thus not give rise to the 10 diffraction peaks in the isointensity plot. It is interesting to notice that the bending rows observed in our quasicrystal could resemble the stripe structure of a spinodal decomposition [7]. Anyhow, in the case of spinodal decomposition, the diffraction pattern would be similar to that of an amorphous structure.

Before concluding, we note that Jagla, using Monte Carlo simulations, recently reported the existence of quasicrystals in a two-dimensional, monodisperse system of hard spheres interacting with a *purely repulsive potential* [4]. The quasicrystal we observe has a different

structure from that modeled by Jagla: our quasicrystal is not a ground state structure and forms only at nonzero temperature. Also, Denton and Löwen have very recently predicted a stable quasicrystal phase in the case of a monodisperse colloidal system [19], in which ionic repulsion combined with polymer-depletion or van der Waals attraction gives rise to a complex radially symmetric interparticle effective potential. To the best of our knowledge, the quasicrystal found in our simulations has a structure different from those previously studied.

We are very grateful to the late Shlomo Alexander, who pointed out the possibility of the formation of quasicrystals in the square-well potential, and we dedicate this work to his memory. We thank R. Hurt and his colleagues at Brown University for encouraging this project in its early stages, L. A. N. Amaral, C. A. Angell, E. Jagla, J. E. McGarrah, C. J. Roberts, R. Sadr, A. Umansky, Masako Yamada for helpful interactions, the DOE for support and the referee for the constructive criticism, and especially F. W. Starr

[1] D. Shechtman, I. Blech, D. Gratias, and J.W. Cahn, Phys. Rev. Lett. **53**, 1951 (1984).

[2] M. Widom, K. J. Strandburg, and R. H. Swendsen, Phys. Rev. Lett. **58**, 706 (1987).

[3] K.W.Wojciechowski, Phys. Rev. B, **46**, 26, (1992).

[4] E. A. Jagla, Phys. Rev. E **58**, 1478 (1998).

[5] S. Narasimhan and M. V. Jaric, Phys. Rev. Lett. **62**, 454 (1989).

[6] A. P. Smith, Phys. Rev. Lett. **63**, 2768 (1989); S. Narasimhan and M. V. Jaric, Phys. Rev. Lett. **63**, 2769 (1989).

[7] P. M. Chaikin, T. C. Lubensky, *Principles of Condensed Matter Physics*, Cambridge University Press, 1995.

[8] D.C.Rapaport, *The Art of Molecular Dynamics Simulation*, Cambridge University Press, 1995.

[9] In constant temperature molecular dynamics, the Berendsen method [proposed by H.J.C Berendsen et al., J. Chem. Phys. **81**, 3684 (1984)] can be used to rescale velocities at each time step by a factor $\chi = \left(1 + \frac{\delta t}{t_T} \left(\frac{T}{\mathcal{T}} - 1\right)\right)^{\frac{1}{2}}$. The current kinetic temperature, \mathcal{T} is rescaled towards the desired temperature T with a rate determined by the time constant t_T . The time step δt is chosen as a constant parameter of the simulation. In our simulation, the velocity rescaling factor takes the same form, except that δt is the average particle collision interval, during which the velocities of all of the particles are rescaled once. Defining our time constant as $t_T = \delta t / \kappa$ allows us to control the quench rate by choosing κ .

[10] To verify the existence of the quasicrystal, we simulated the same density in a smaller system of 529 particles. At $T = 0.2$, the 10 five-fold diffraction peaks appeared, giving evidence to the formation of the quasicrystalline phase.

[11] Time units are defined so that $T = \langle mv^2/2 \rangle$. For our parameters of N, V, and T=0.1, we

find that the average collision interval is approximately one time unit.

[12] To form the amorphous phase from the high temperature liquid, a quench rate of $\kappa = 1$ is used. The amorphous phase is annealed at a slower quench rate of $\kappa = 0.01$.

[13] A.P.Tsai, MRS Bulletin, **22**, 43 (1997).

[14] C. Kittel, *Introduction to Solid State Physics*, John Wiley and Sons, Inc., 1996.

[15] For $\rho = 0.857$, pressure at this density is almost constant, as energy continually decreases (Fig. 6). For densities slightly below or above $\rho = 0.857$, pressure suffers a constant drift during the time scales accessible to our simulations, indicating that the system, at these densities, is further from equilibrium than when $\rho = 0.857$.

[16] Two large defects appear in 4c, one at the bottom center and the other in the upper right quadrant.

[17] T. M. Birshtein and S. V. Buldyrev, Polymer **32**, 3387 (1991).

[18] M. Senechal, *Quasicrystals and Geometry* (Cambridge University Press, Cambridge, 1995).

[19] A. R. Denton and H. Löwen, cond-mat/9803078.

TABLE I. Energy U , entropy S and the Helmholtz potential A at temperature $T = 0.2$ where the quasicrystal is found

Crystal	U	S	$A(T = 0.2)$
Pentagonal I	$-4\frac{2}{5}$	1.259 ± 0.028	-4.652
Pentagonal II	$-4\frac{1}{3}$	1.603 ± 0.0052	-4.654
Square	-4	3.247 ± 0.021	-4.649

FIG. 1. The square-well potential. The ratio of the attractive distance b to the hard core repulsive distance a is $b/a = \sqrt{3}$. The depth of the square-well $\epsilon = -1.0$ is the interaction energy per pair of particles.

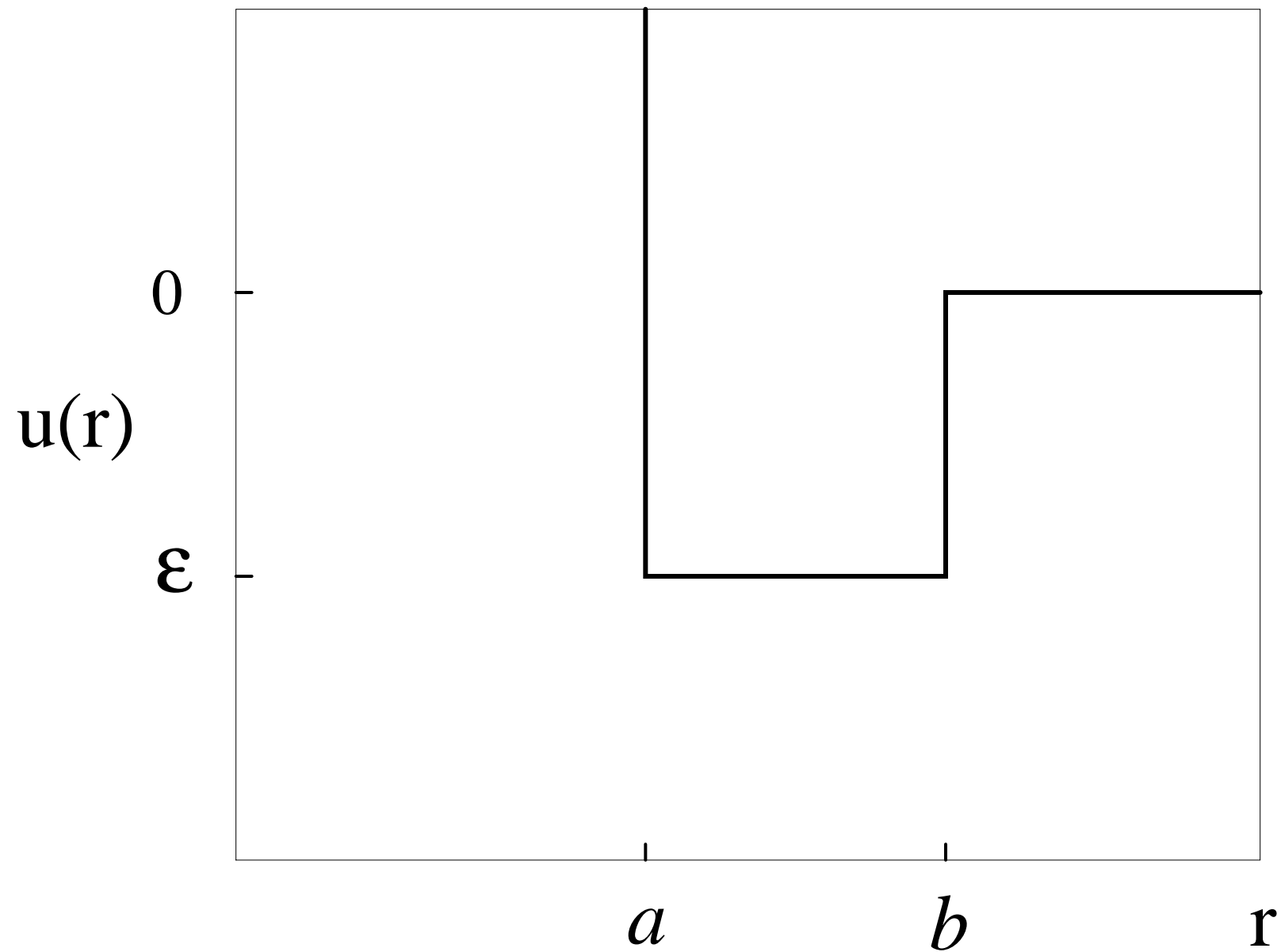
FIG. 2. Repeating segments of the three crystals. (a) In the square crystal, each particle interacts with 8 nearest neighbors. The square crystal is constituted by particles interacting with a square geometry. (b) In type I pentagonal crystals, $\frac{1}{5}$ of the particles have 8 neighbors and $\frac{4}{5}$ of the particles have 9 neighbors. (c) In type II pentagonal crystals, $\frac{1}{3}$ of the particles have 8 neighbors and $\frac{2}{3}$ of the particles have 9 neighbors. Five particle pentagons, denoted by letter “P”, form the pentagonal crystals. The particles indicated in white are the particles in a basic cell that can be used to construct the crystal by translation; there are respectively one, five and six particles in the unit cell of the square, pentagonal I and pentagonal II crystals.

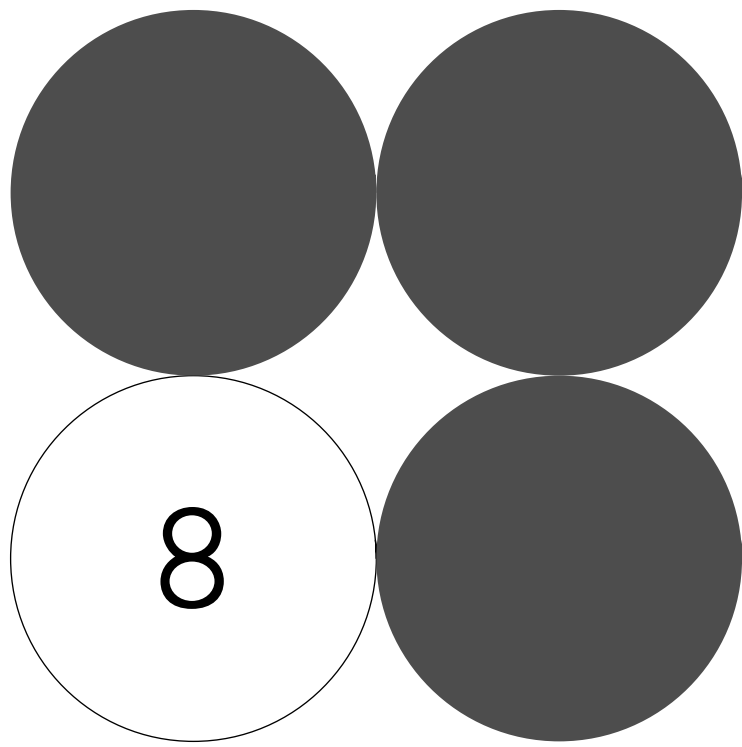
FIG. 3. The Helmholtz potentials of pentagonal crystals of type I and II and the square crystal at various temperatures. Points A, B, and C, of the inset, indicate the intersections of the Helmholtz potential lines at $T_A = 0.195 \pm 0.010$, $T_B = 0.201 \pm 0.005$, $T_C = 0.203 \pm 0.006$. The solid line indicates the lowest Helmholtz potential: below T_A the type I pentagonal crystal is the most stable, between T_A and T_C the type II pentagonal crystal is the most stable, and above T_C the square crystal is the most stable.

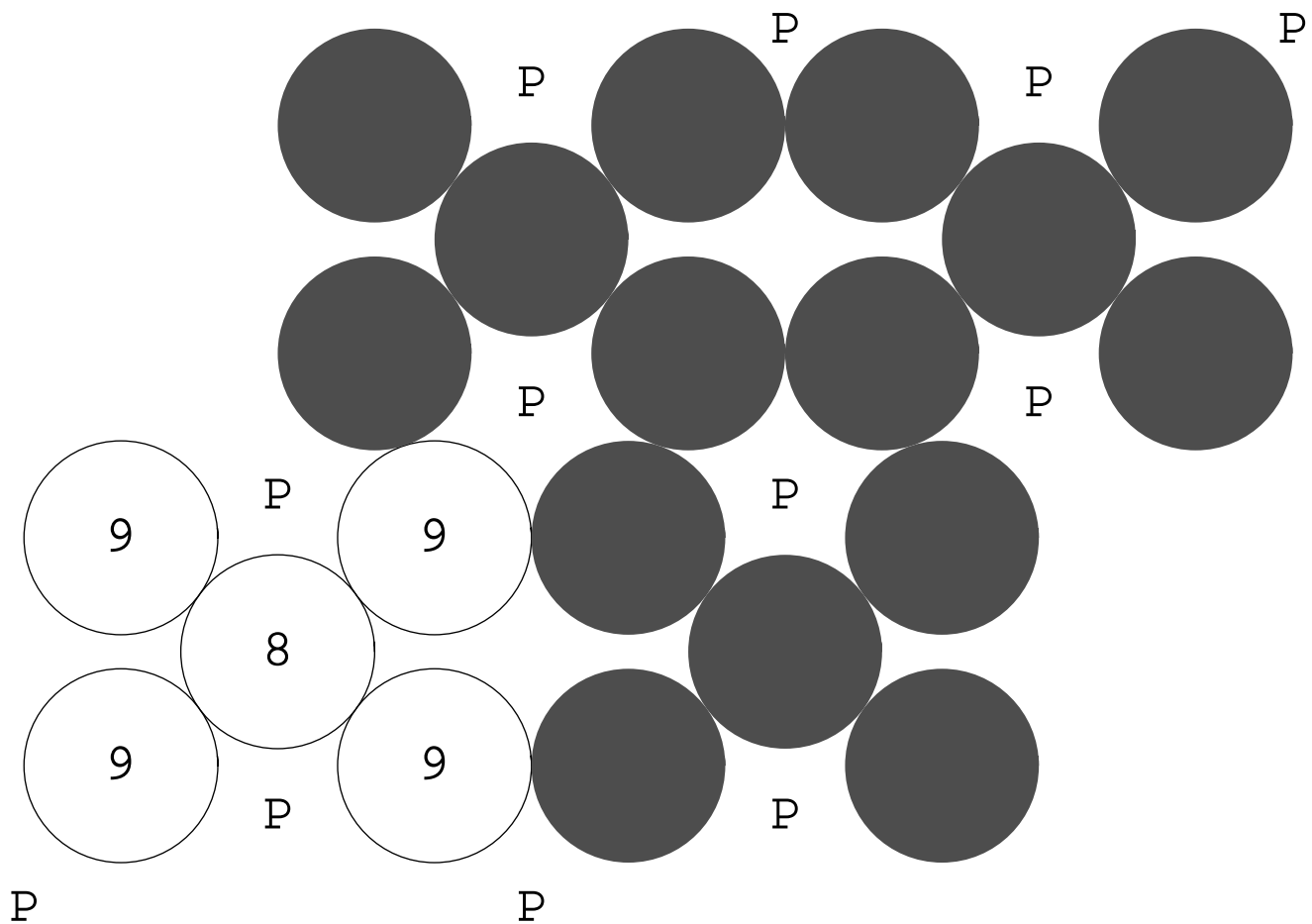
FIG. 4. Amorphous and quasicrystal phases are shown along with their corresponding isointensity plots: the simulated equivalent to a crystallographic diffraction pattern, given by the Fourier transform of the density function: the darkness is proportional to the amplitude of the Fourier transform. Pentagons are indicated by the shaded areas and lines indicate the interaction between centers of particles. (a) Uniformly distributed pentagons in the amorphous phase give rise to the (b) homogeneous rings in the isointensity plot. (c) The pentagons in the quasicrystal phase have coalesced in curved rows that run approximately parallel to one another, in contrast to part (a) where the rows are much less apparent and are not even approximately parallel. (d) The ten isointensity peaks of the quasicrystal.

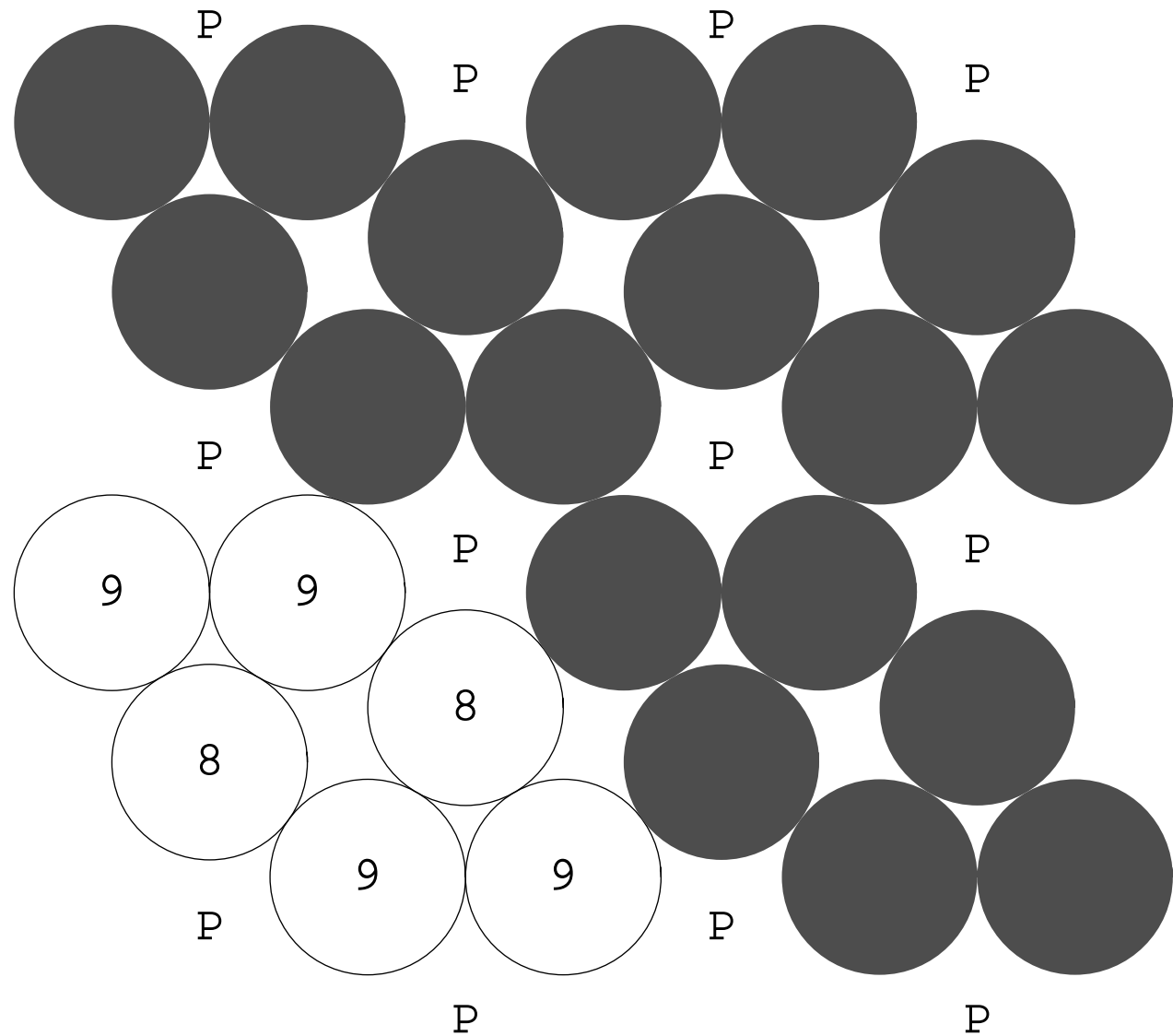
FIG. 5. The (a)square crystal, (b) type I pentagonal crystal and (c) type II pentagonal crystal isointensity plots.

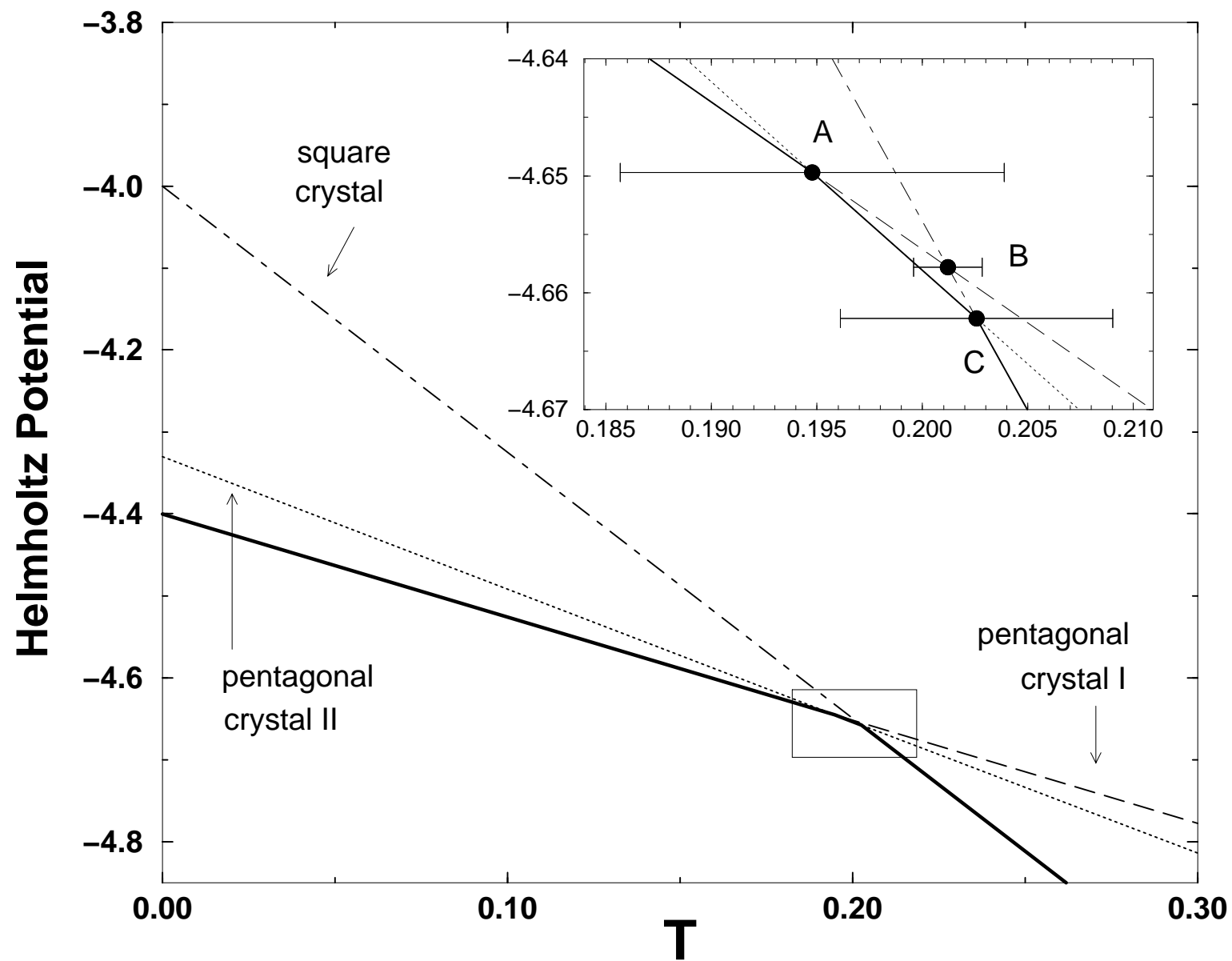
FIG. 6. Behavior of P , U and D versus time when the system, initially in the amorphous phase, is equilibrated at $T = 0.205$. The density is $\rho = 0.857$ and the number of particles is $N = 961$



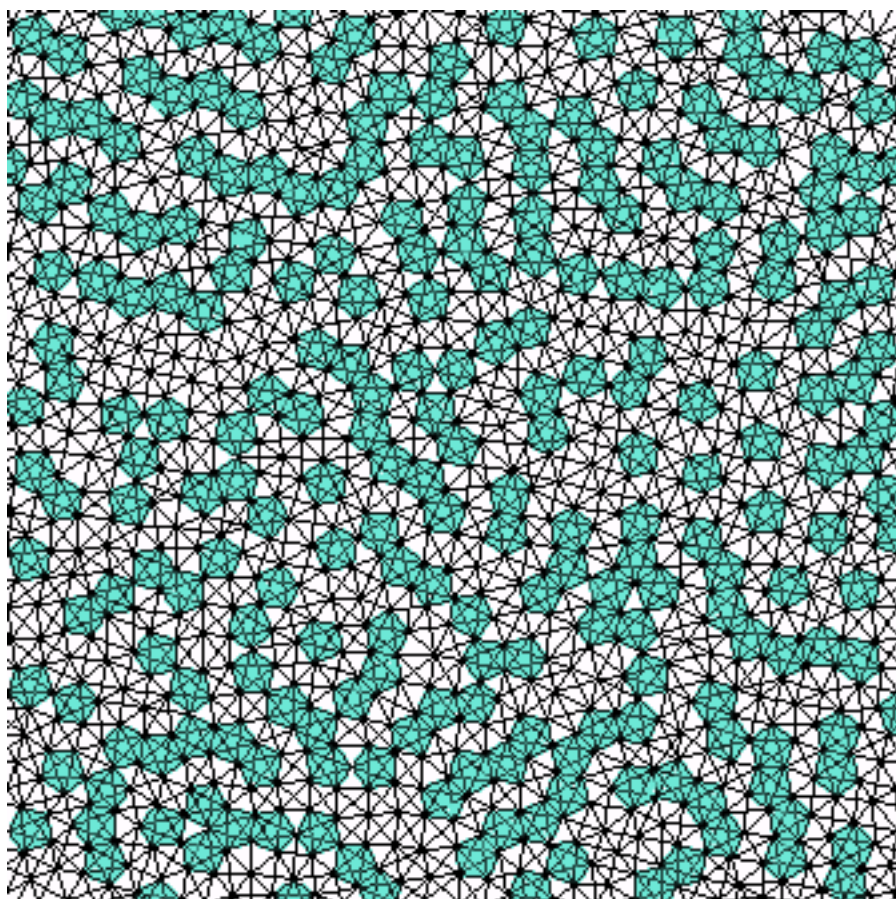




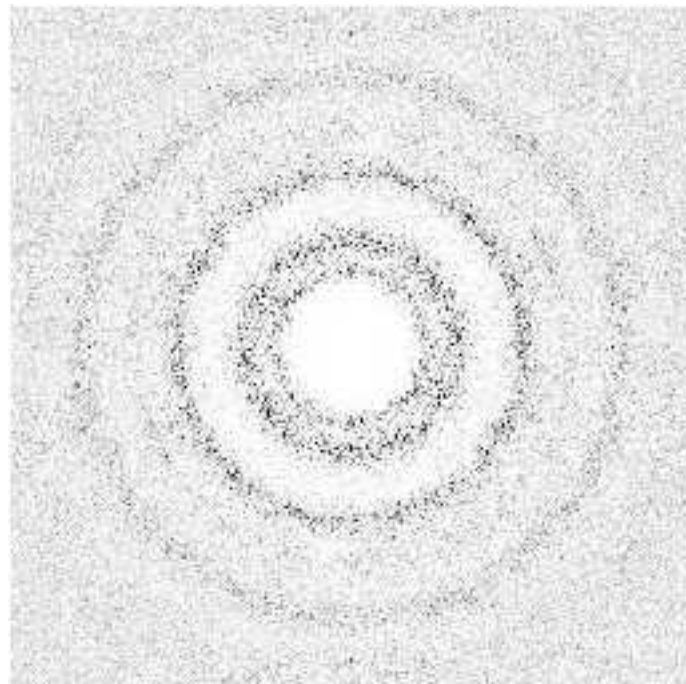




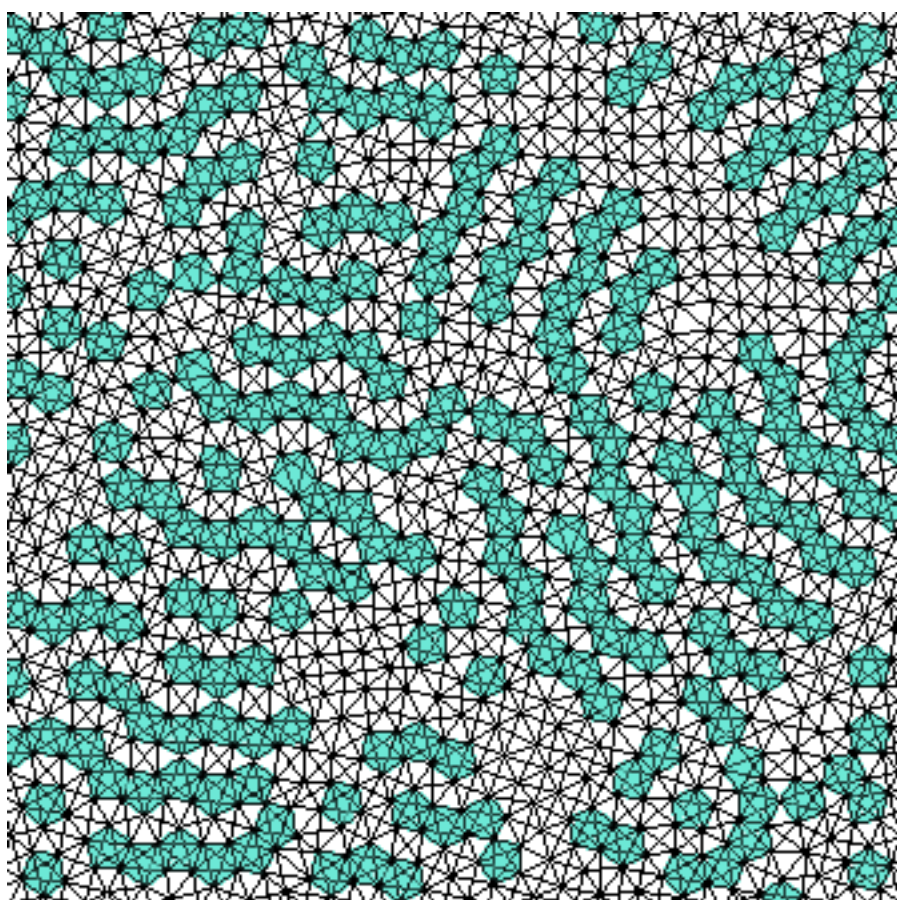
(a)



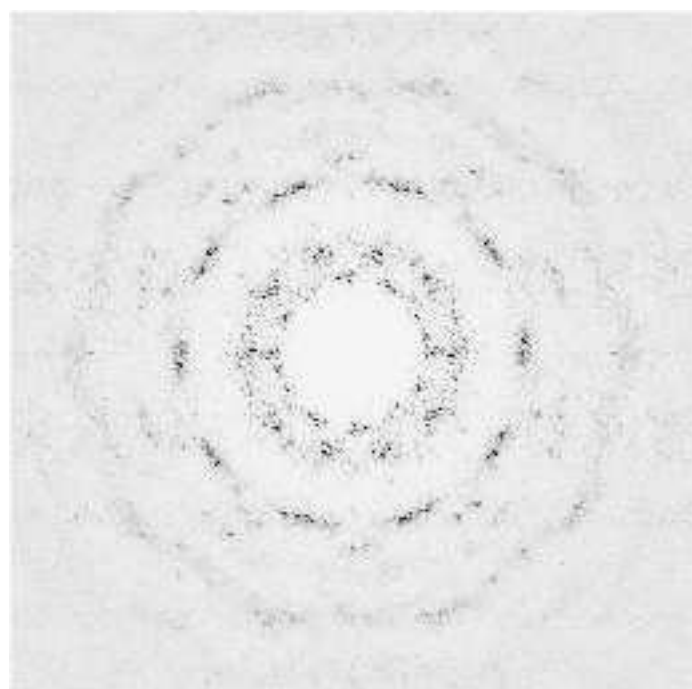
(b)

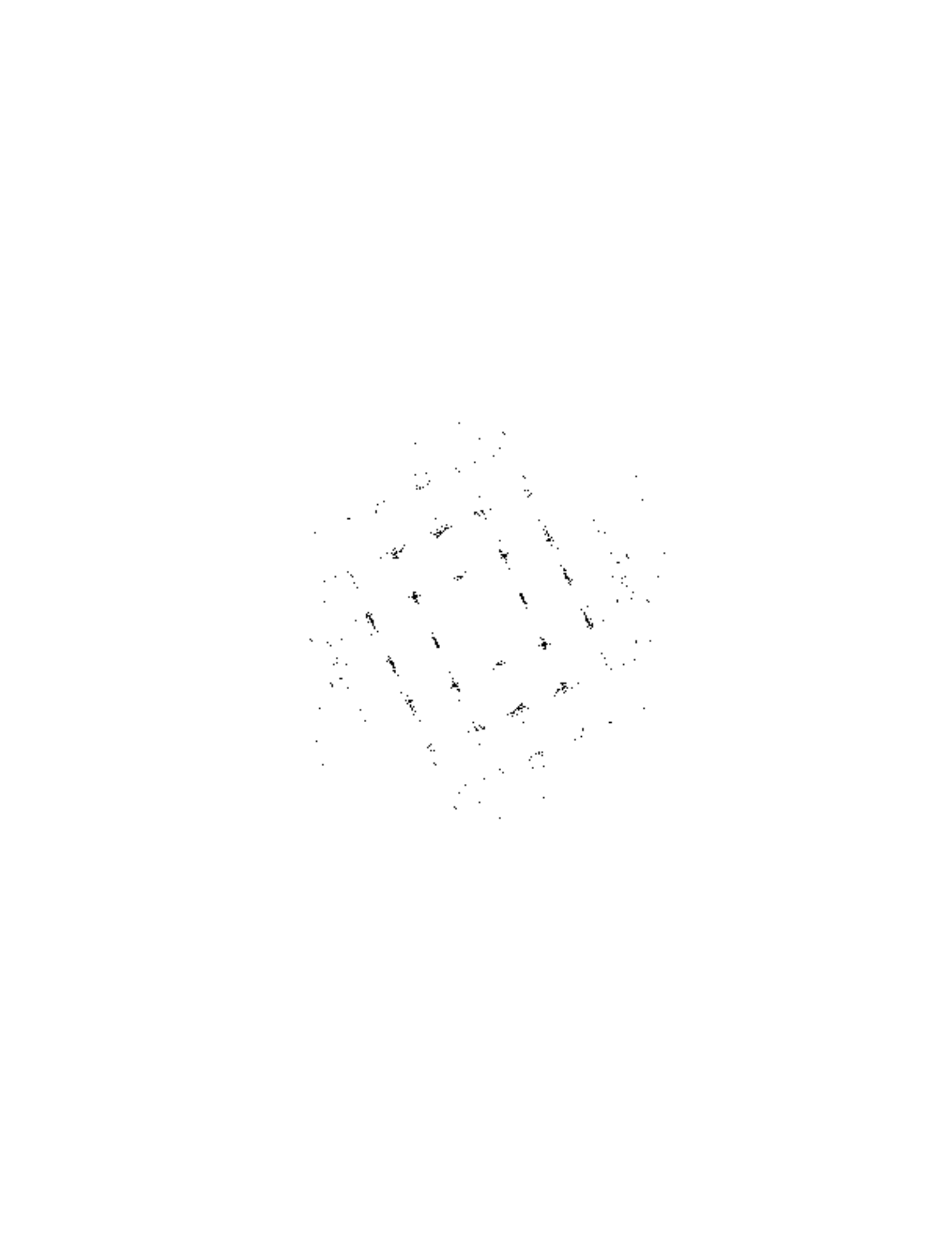


(c)



(d)





1. *Neuroleptic-induced hypomania* is a well-known side effect of neuroleptic drugs. It is often associated with the use of atypical neuroleptics, such as risperidone, olanzapine, and quetiapine. The mechanism of action is not fully understood but may involve the blockade of serotonin 5-HT₂ receptors. Clinical presentation includes elevated mood, increased energy, and reduced need for sleep. Treatment typically involves discontinuing the neuroleptic and switching to a different class of medication.

2. *Neuroleptic-induced akathisia* is a movement disorder characterized by a strong urge to move, often described as a "need to move" or "restlessness." It is most commonly associated with the use of typical neuroleptics, such as haloperidol and chlorpromazine. The mechanism of action is thought to be the blockade of dopamine D₂ receptors in the mesolimbic and mesocortical pathways. Treatment may include switching to an atypical neuroleptic or adding a dopamine agonist, such as bromocriptine or pergolide.

3. *Neuroleptic-induced dystonia* is a movement disorder characterized by involuntary muscle contractions, often involving the neck, jaw, or eyes. It is most commonly associated with the use of typical neuroleptics, such as haloperidol and chlorpromazine. The mechanism of action is thought to be the blockade of dopamine D₂ receptors in the extrapyramidal system. Treatment may include discontinuing the neuroleptic or adding a dopamine agonist, such as bromocriptine or pergolide.

4. *Neuroleptic-induced sedation* is a common side effect of neuroleptics, particularly typical neuroleptics. It can lead to drowsiness, fatigue, and difficulty concentrating. The mechanism of action is thought to be the blockade of dopamine D₂ receptors in the mesolimbic and mesocortical pathways. Treatment may include discontinuing the neuroleptic or switching to an atypical neuroleptic.

5. *Neuroleptic-induced constipation* is a common side effect of neuroleptics, particularly typical neuroleptics. It can lead to difficulty passing stool and can be a source of discomfort and distress. The mechanism of action is thought to be the blockade of dopamine D₂ receptors in the gut. Treatment may include discontinuing the neuroleptic or adding a laxative, such as stool softener or a fiber supplement.

